Pharm Res (2012) 29:2845–2859
DOI 10.1007/s11095-012-0779-4

RESEARCH PAPER

New Respirable and Fast Dissolving Itraconazole Dry Powder Composition for the Treatment of Invasive Pulmonary Aspergillosis

Christophe Duret • Nathalie Wauthoz • Thami Sebti • Francis Vanderbist • Karim Amighi

Received: 9 March 2012 / Accepted: 11 May 2012 / Published online: 30 May 2012

ABSTRACT

Purpose Novel itraconazole (ITZ)-based dry powders for inhalation (DPI) were optimized for aerodynamic and dissolution properties and contained excipients that are acceptable for inhalation.

Methods The DPI were produced by spray drying solutions. The drug content, crystallinity state, and morphological evaluation of the dry powders were determined by high performance liquid chromatography, powder X-ray diffraction, differential scanning calorimetry, and scanning electron microscopy, respectively. A particle size analysis was conducted using laser light scattering. The aerodynamic behaviors of the powders were characterized by impaction tests. ITZ dissolution rates were evaluated using a dissolution method adapted to inhaled products.

Results The DPI presented very high fine particle fractions that ranged from 46.9% to 67.0% of the nominal dose. The formulations showed very fast dissolution rates compared to unformulated crystalline ITZ with the possibility of modulating the dissolution rate by varying the quantity of phospholipids (PL) incorporated. ITZ remained amorphous while the mannitol was crystalline. The α, β and δ-mannitol polymorph ratios varied depending on the formulation compositions.

Conclusion This formulation strategy could be an attractive alternative for treating invasive pulmonary aspergillosis. The ITZ and PL content are key characteristics because of their influence on the dissolution rate and aerosol performance.

C. Duret (✉) · N. Wauthoz · K. Amighi
Laboratoire de Pharmacie Galénique et de Biopharmacie
Université Libre de Bruxelles
Boulevard du Triomphe - CP207 Campus de la Plaine
1050 Brussels, Belgium
e-mail: cduret@ulb.ac.be

T. Sebti · F. Vanderbist
Laboratoires SMB S.A.
26-28 Rue de la Pastorale
1080 Brussels, Belgium

KEY WORDS dry powder for inhalation (DPI) · invasive aspergillosis · itraconazole · mannitol · polymorphism

ABBREVIATIONS

API	active pharmaceutical ingredient
CI	Carr's index
d_{ae}	aerodynamic diameter
DPI(s)	dry powder(s) for inhalation
ED	emitted dose
FDA	Food and Drug Administration
FPD	fine particle dose
FPF	fine particle fraction
IA	invasive aspergillosis
IC	immunocompromised
ICDD	International Center for Diffraction Data
ITZ	itraconazole
IV	intravenous
MIC	minimal inhibitory concentration
MsLI	multi-stage liquid impactor
MTDSC	modulated temperature differential scanning calorimetry
NGI	next generation impactor
PL	phospholipids
PSD	particle size distribution
PXRD	powder X-ray diffraction
RIR	reference intensity ratio
RPM	round per minute
SD	spray dried
SEM	scanning electron microscopy
TGA	thermogravimetric analysis

INTRODUCTION

Aspergillosis refers to the spectrum of pathologies caused by *Aspergillus* species. These species are filamentous fungi, more

precisely ascomycetes. Invasive aspergillosis (IA) is an advanced state of *Aspergillus* colonization that occurs after the germination of conidia. IA is a frequent cause of infectious disease related to morbidity and mortality in immunocompromised (IC) patients. In the past two decades, the incidence of IA infections has increased dramatically. For instance, from the 1980s to 1997, the trend in mortality associated with IA increased by 357% (1). Because aspergillosis is an opportunistic disease, this rise in IA frequency can be explained by the rising number of IC patients currently encountered in clinical practice.

Similar to all ascomycetes, *Aspergillus* reproduces by the production of conidia, which can remain suspended in the air and survive out in the open for long periods of time. The hosts are most commonly contaminated with these conidia by inhalation. The lungs are the principal gateway for this pathogen (80–90% of IA (2)) and are often the starting point for the invasion, which can lead to lethal dissemination in more than 90% of cases (2). As previously reported, the invasive state is mainly reached in the IC population, in which the immune defenses (principally macrophages and neutrophils (3)) are not sufficiently strong to prevent the germination of conidia after inhalation. Consequently, the hyphae proliferate through the tissues and blood capillaries in the contaminated area, reaching what is commonly called the invasive state.

Despite the current advanced therapies, the mortality rate is still very high (from 40% to 90%) when the invasive stage is reached (this number varies depending on the patient category and study). For most IC patients, progression can be dramatically fast (e.g., 7–14 days from onset to death) (2). This high rate of treatment failure can be explained by the combination of several factors. First, depending on the symptoms that are presented, invasive pulmonary aspergillosis is difficult to diagnose in the first stage of the disease. By the time the first clinical manifestations of the infection occur (i.e., hemoptysis), the invasive state has often already been reached. Another important reason for treatment failure is that the existing therapies are administered orally and/or intravenously and can induce a large number of side effects and metabolic interactions (4) because of the high systemic concentrations needed to achieve an effective pulmonary concentration. Moreover, due to the poor solubility of these antifungal drugs, oral therapies show high inter- and intra-individual variation in terms of bioavailability, which may lead to infra-therapeutic concentrations in the lung tissue and therefore inside the fungal lesion (5). For these reasons, pulmonary delivery constitutes an interesting alternative for prophylaxis and/or the treatment of invasive pulmonary aspergillosis. Delivering antifungal medication directly to the lung at the infection site allows concentrations above the minimal inhibitory concentration (MIC) 90% to be effectively and directly maintained in the lung tissue. This approach was found to be effective in some preclinical trials (6,7). Bypassing the systemic circulation should minimize the occurrence of side effects and metabolic interactions that are often the reason for antifungal treatment failure.

In the present study, ITZ, a broad-spectrum antifungal agent, was chosen as the active pharmaceutical ingredient (API) to be formulated as a dry powder and administered by inhalation in the treatment strategy described above. This API has already shown attractive properties in terms of efficacy and safety in previous mouse studies investigating pulmonary IA prophylaxis by inhalation (nebulization) (6,7). DPIs have received considerable attention for pulmonary drug delivery in the past few years. This attention is due to their numerous advantages, such as their propellant-free composition, increased long-term storage stability, and passive actuation, compared to metered dose inhalers and nebulizers (8).

The formulation strategy for a DPI including an active ingredient such as ITZ involves several specific considerations. The formulation should be characterized by a suitable aerodynamic particle size distribution to achieve effective lung deposition after dose actuation from an inhaler device. More precisely, the API deposition profile has to be considered in relation to the aerodynamic diameter (d_{ae}) of the potentially inhaled conidia. Indeed, the d_{ae} of the conidia will determine their deposition site in the lung and therefore the fungal germination and infiltration sites. ITZ is a poorly water-soluble API classified in class II of the Biopharmaceutical Classification System (9), and its dissolution rate is a limiting factor for its efficacy (10) and safety (local irritation and inflammation) when administered through the pulmonary route (11,12). For these reasons, the formulation design should include a pharmaceutical strategy to improve drug dissolution. Enhancing drug dissolution and solubility should also allow a higher quantity of drug to diffuse through the pulmonary epithelium directly to sites where the fungus could have infiltrated. There are several strategies for improving drug dissolution and/or solubility (13). However, the field of action is considerably restricted in pulmonary drug delivery due to the low number of FDA-authorized inactive ingredients/solvents that can be used in both the manufacturing process and the composition of the developed product (14).

To optimize the dissolution rate of ITZ while maintaining good aerodynamic performance, we decided to produce solid dispersions with excipients acceptable for inhalation. In a previous study, we showed the ability to improve the ITZ dissolution rate and saturation solubility when those solid dispersions were composed of a mannitol matrix in which ITZ was dispersed in a glassy amorphous form (15). However, we found that the addition of a surfactant, tocopherol polyethylene glycol 1000 succinate (TPGS), accelerated the ITZ dissolution rate and improved the saturation solubility but dramatically decreased the aerosolization properties. To

maintain this acceleration of dissolution using an accepted excipient and not affecting aerosol performance, we decided to develop ITZ-based solid dispersions with mannitol and the hydrogenated soy-lecithin present in the lung as a surfactant. These new formulations could represent an attractive alternative for combating IA by localized delivery. Localized delivery of this formulation type would allow the API concentration in the lung to be maximized and the systemic exposure to be minimized, which drastically decreases the possibility of systemic side effects and metabolic interactions. The aim of this study was to evaluate those new compositions in term of dissolution and aerosolization. A particular attention was paid on particles polymorphism.

MATERIALS AND METHODS

Materials

Raw ITZ was purchased from Hetero Drugs Ltd. (Andhra Pradesh, India) and micronized by jet milling (volume mean diameter, 3.5 μm; 90% of particles below 6.2 μm). The Phospholipon 90 H®, which is composed of hydrogenated soy-lecithin with more than 90% hydrogenated phosphatidylcholine, was purchased from Nattermann Phospholipids GmbH (Köln, Germany). The Pearlitol PF® (mannitol) was kindly donated by Roquette Frères (Lestreme, France). The sodium lauryl sulfate was purchased from Sigma Aldrich (Belgium). All of the solvents used were analytical grade.

Methods

Dry Powder Preparation

The dry powders were produced by spray-drying using a Büchi mini spray-dryer B-191a (Büchi Laboratory-Techniques, Switzerland). Spray-drying is a useful technique in DPI production because of its easy operation and the opportunity for controlling particle size distribution, density, and morphology by modification of the formulation and atomization parameters (16). The solutions were prepared as follows. ITZ and the excipient(s) were dissolved under magnetic stirring (600 rpm) in a hydro-alcoholic solution (water-isopropanol 20:80) heated to 70°C. The solutions were then spray-dried under the following conditions to retrieve dry particles: spraying air flow, 800 L/h; drying air flow, 35 m^3/h; solution feed rate, 2.7 g/min; nozzle size, 0.5 mm. The compositions of the spray-dried hydro-alcoholic solutions are summarized in Table I. The different solutions were spray-dried at an inlet temperature fixed at 90°C, generating an outlet temperature of 55°C, which was found to be the upper limit of the outlet temperature for preventing glassy ITZ liquefaction (15).

Characterization of Crystallinity

The crystallinity profile of each sample was assessed using modulated temperature differential scanning calorimetry (MTDSC) and powder X-ray diffraction (PXRD). These two techniques provide complementary information on polymorphisms.

MTDSC. The MTDSC experiments were conducted using a Q 2000 DSC (TA Instruments, Zellik, Belgium) equipped with a refrigerated cooling system. Crystallization phenomena were observed in the non-reversing heat flow, glass transformations were observed in the reversing heat flow, and melting was observed in the total heat flow. All of the samples were analyzed in the same conditions, which follow. A 2–3 mg sample was precisely weighed in a low mass hermetic aluminum pan. The sample was heated from 25°C to 185°C at a 5°C/min temperature rate with a modulation of +/−0.8°C every 60 s. The instrument was calibrated for temperature using indium. The heat flow and heat capacity signals were calibrated using a standard sapphire sample. Universal Analysis 2000 software was used to integrate each thermal event.

PXRD. The powders were analyzed using the Debye-Scherrer method. The samples were passed under the Kα line of copper with monochromatic radiation (λ=1.540 Å). The diffractometer (Siemens D5000, Germany) was equipped with a mounting for Bragg-Brentano reflection and connected to a monochromator and the Diffracplus channel program. The measurements were made at 40 kV and 40 mA with an angular 2θ range from 2° to 60° in steps of 0.02°, a counting speed of 1.2 s per step and a sample rotation speed of 15 rpm.

The percentage of crystalline phase in the spray-dried powders was measured using the surface area ratio method (17). The degree of crystallinity was calculated as in equation 1, where A_T is the total area under the diffractogram and A_c is the area under the diffractogram without integrating the deviation from the baseline. The amorphous content (expressed in %) was estimated as 100% minus the estimated degree of crystallinity.

$$\%Crystallinity = \left(\frac{A_C}{A_T}\right) \times 100$$

The reference intensity ratio (RIR) technique (18–20) was used to investigate the polymorphism of mannitol after spray-drying. This semi-quantitative method of estimation consists of comparing the peak intensities of the different phases in a specimen with reference patterns (from the database of the International Center for Diffraction Data,

Table I Theoretical Composition of the Spray-Dried Solutions in Water-Isopropanol (80:20) and the Dry Powder Formulations

Sample	Solution composition			Dry powder composition		
	ITZ % (w/v)	Mannitol % (w/v)	PL % (m/m_{ITZ})	ITZ % (w/w)	Mannitol % (w/w)	PL % (w/w)
F1	0.56	1	–	35.9	64.1	–
F2	0.1	0.9	–	10	90	–
F3	0.56	1	1	35.77	63.87	0.36
F4	0.56	1	10	34.65	61.88	3.47
F5	0.1	0.9	10	9.90	89.11	0.99
Spray-dried ITZ	0.56	–	–	100	–	–
Mannitol	–	1	–	–	100	–

ICDD). One specific diffraction peak was chosen for each polymorph (when there was no other crystalline structure that could be present in the diffracted dry powder); specific diffraction peaks at 43.92, 16.81, and 22.09° 2θ were used for α-, β-, and δ-mannitol, respectively, and their respective ICDD spectrums were adjusted to those diffraction rays for the calculation. The calculations were made using the Diffracplus EVA software (Bruker Belgium S.A., Brussels, Belgium). The results are expressed as an estimation of the percentage of each polymorph in the formulations.

Characterization of Flow Properties

The Carr's compressibility index (CI) was used to evaluate powder flowability. A pre-weighed quantity of dry powder was placed in a 10 ml graduated cylinder. The apparent volume occupied by the powder was noted before and after the application of 1000 taps to the cylinder using a tap density tester (Stampfvolumeter, STAV 2003, Jel, Germany). The CI was then calculated from the difference between the apparent volume before and after tapping and was expressed as the percentage of apparent volume before tapping, as described in European Pharmacopoeia 7.2. CI values below 25% are usually taken to indicate good flowability, whereas values above 40% indicate poor flowability.

Thermogravimetric Analysis

The residual moisture and solvent content of the different dry powders was assessed using thermogravimetric analysis (TGA) with a Q500 apparatus (TA instruments, New Castle, USA) and Universal Analysis 2000 software version 4.4A (TA Instruments, Zellik, Belgium). The residual water and solvent content was calculated as the weight lost between 25°C and 125°C and was expressed as a percentage of the initial sample mass. The runs were set from 25°C to 300°C at a heating rate of 10°C/min on a sample mass of about 10 mg and were performed in triplicate.

Characterization of Particle Shape by Scanning Electron Microscopy

The morphology of the particles was evaluated using an environmental scanning electron microscope (Philips XL30 ESEM-FEG; FEI, Eindhoven, the Netherlands). The samples were spread on a carbon adhesive band and coated with gold at 40 mA and 6.10^{-2} mbar for 90 s under argon. Observations were made at an acceleration between 3 kV and 25 kV, depending on the sample.

Particle Size Analysis

The particle size distribution (PSD) of the dry powders was evaluated by laser scattering using a Malvern Mastersizer 2000® equipped with a Sirocco® dry feeder dispersion unit (Malvern Instruments Ltd, Worcestershire, UK). The particle size measurements were carried out on a sample of about 50 mg at a pressure of 4 bars and a feed rate vibration set at 40%. These conditions allowed the measurement of the PSD of almost completely deagglomerated powder due to the very drastic dispersion conditions that were generated in the dispersion unit. A particle refractive index with a real part of 1.48 and imaginary part of 0.1 were chosen for the formulation, while values of 1.61 and 0.01 were used for pure ITZ. These values ensured a low-weighted residual (<2%), which ensures the integrity of results.

A Malvern Spraytec® (Malvern Instruments Ltd, Worcestershire, UK) was used to measure the PSD of the aerosol cloud that penetrated the MsLI during particle aerodynamic behavior analysis. The laser beam was placed directly between the throat and the impactor to measure the PSD of the dry powder cloud generated. The dry powder cloud was fractionated as a function of its d_{ae} in the MsLI during simulated inhalation conditions. For both techniques, the average PSD was

calculated from three replicate measurements of each sample. The results were expressed in terms of D[4,3] and d(0.5), which are the mean volume diameter and the median volume diameter (the size in microns at which 50% of the particles are smaller than the rest of the distribution), respectively.

Particle Aerodynamic Behavior Analysis

The particle aerodynamic behavior analyses were conducted using a multi-stage liquid impinger (MsLI, Copley Scientific, Nottingham, England). An Axahaler® (Laboratoires SMB, Belgium) was used as the dry powder inhaler. A flow rate (adjusted to a pressure drop of 4 kPa) of 100 L/min for 2.4 s was applied throughout the device for dose actuation. At this flow rate, the particles with a d_{ae} above 10 μm were stopped in the connection port, while the particles with a d_{ae} between 10 and 5.27 μm were stopped in the two first stages of the MsLI. The cut-off diameters were 5.27, 2.40, and 1.35 μm between stages 2 and 3, 3 and 4, and 4 and 5, respectively. The flow rate was measured using a DFM3 flow meter (Copley Scientific, Nottingham, United Kingdom). The device was filled with n°3 HPMC capsules (Qualicaps, Spain) that were loaded with an approximate quantity of dry powder corresponding to 2.5 mg of ITZ. Three capsules were used for one test. After the three dose actuations, the total amount of dry powder deposited in each part of the impactor was quantified using a suitable and validated HPLC method. Each test was repeated three times. The fine particle dose (FPD), fine particle fraction (FPF), and emitted dose (ED) were calculated for each formulation. The FPD corresponds to the mass of the active substance with a d_{ae} smaller than 5 μm. The FPD was determined by interpolation from the cumulative mass *versus* the cut-off diameter of the respective stage. The FPF is the FPD expressed as a percentage of the nominal dose, while the ED corresponds to the percentage of the total drug dose that was recovered in the throat, stages 1, 2, and 3, and the filter of the MsLI during the tests.

Drug Content Determination

The drug content was determined to compare the expected and actual drug content. The samples were reconstituted in an appropriate solvent and analyzed using an HPLC quantification method. The average content (% by weight of dry form, wt %), relative standard deviation percentage (RSD%), and relative errors were calculated from five analyses.

Dissolution Tests

The dissolution performances were evaluated using a specific dissolution method that was recently developed for DPI. A device was designed to collect a dry powder dose exhibiting a determined aerodynamic range on a flat surface after actuation from an inhaler device (15). The device consists of a dose collector plate (called the membrane cassette) that is fixed on a quick release plate and placed on stage 3 of a Next Generation Impactor (NGI) (Copley Scientific Limited, Nottingham, UK). After the dose actuation from an inhaler device into the NGI, the membrane cassette was removed, covered with a polycarbonate membrane (0.4 μm diameter pore) (Millipore, Ville, Pays), and sealed in place with a sealing ring. This prepared dose collector device was then placed in the bottom of a dissolution vessel with a paddle apparatus (USP 33 type 2 apparatus, Erweka DT6, Heusenstamm, Germany), and the dissolution testing was conducted as described below. Once the collector device was placed in the dissolution vessel, the following conditions were used. The paddle speed was set at 75 rpm, and the dissolution vessel was filled with 300 ml of dissolution media. Itraconazole release was quantified at pre-determined intervals (0, 2, 5, 10, 20, 30, 60, 120, and 180 min) with a suitable HPLC method. For this quantification procedure, volumes of 2 ml of the dissolution media were removed from the dissolution vessel at different time intervals and directly replaced with fresh dissolution medium. These 2 ml samples were directly filtered through 0.2 μm diameter filters to avoid the quantification of undissolved particles at the determined time intervals. The cumulative amount of drug released was calculated, expressed as a percentage of the total drug load and plotted *versus* time. At the end of the test, the dose collection plate was removed from the dissolution vessel and washed with an exact volume of dilution phase for the quantification of the undissolved fraction. An Axahaler® device (SMB®, Brussels, Belgium) containing a n°3 HPMC capsule (Qualicaps®, Madrid, Spain) was used as the inhaler. The dose actuations were realized once per insert at a flow rate of 60 L/min for 4 s. The nominal doses were adapted for a total ITZ load dose of about 400 μg on each insert. Each test was repeated three times. In these conditions, the d_{ae} range of the collected particles was between 2.82 and 4.46 μm. This measurement was performed to evaluate whether the particles exhibiting the same d_{ae} as potentially inhaled conidia (~3 μm) (21) presented an improved dissolution rate. The dissolution media was a physiological buffered solution that was described in European Pharmacopoeia 7.2 (pH adjusted to 7.2). Sodium lauryl sulfate (0.3%) was added to this solution to reach sink conditions. The physiological buffered solution was composed (w/v) of 0.8% sodium chloride, 0.02% potassium chloride, 0.01% calcium chloride, 0.01% magnesium chloride, 0.318% disodium hydrogen phosphate and 0.02% potassium dihydrogen phosphate. The media was heated to 37°C and maintained at this temperature throughout the tests.

HPLC/UV Method

A suitable validated HPLC/UV method was used to quantify ITZ. The analyses were performed using an HP 1200 series (Agilent Technologies, Brussels, Belgium) equipped with a

binary pump, an autosampler, and a diode array detector with a detection wavelength set at 263 nm. The separations were performed in reverse phase using a LiChroCART Purospher® Star RP 18 (N-capped), which is a base-deactivated column (5 μm) (Merck Chemical, Overijse, Belgium). The mobile phase (acetonitrile-phosphate buffer adjusted to pH 6.4, 60:40) was run at a flow rate of 1 ml/min.

Statistical Analysis

The dissolution data releases obtained were statistically compared using the fit factor (22), as recommended by the FDA's Guidance for Industry. The difference and similarity fit factors (f_1 and f_2) were calculated to compare pairs of dissolution profiles. The curves were considered similar if the f_1 value was below 15 and the f_2 value was close to 100 (between 50 and 100).

RESULTS AND DISCUSSION

Physicochemical Characterization

The ITZ content results for the different formulations are summarized in Table II. The measured values were very close to the expected values, with relative errors ranging between −3.9% and 3.0%. The active ingredient seemed to be uniformly distributed, as the RSD% remained within reasonable limits (less than 3.3%). A good API distribution in the particles is a crucial point for uniformity in the administered dose. The measured ITZ content values were used as the nominal doses during the aerodynamic fine particle assessment. The relative error between the measured and expected ITZ content for pure spray-dried ITZ (100%) was equal to 0.7%.

TGA analysis was used to assess the residual water and isopropanol remaining after the spray-drying process. After that the samples were heated from 25°C to 125°C, the measured weight losses were very low (<0.5%, Table II) for each formulation. These low values indicate almost complete solvent and water evaporation during the spray-drying process. Low residual water and solvent contents are important for reducing both toxicity risks and the agglomeration of particles by capillary interactions during inhalation (23), in addition to enhancing product stability during long-term storage (24).

After spray-drying a solution, it is possible that different polymorphic forms or polymorph mixtures, as well as amorphous material, may be obtained in the final dry product. Because the solubility, activity, stability, morphology, and physicochemical properties of a compound can be modified by its polymorphic form, it is important to fully characterize it. PXRD and MTDSC are two widely used, complementary techniques that help to determine the crystalline properties of a solid.

Following the conditions described above, spray-dried ITZ was retrieved in its dry, amorphous, glassy state and was characterized by specific thermal events (15). This particular profile was also observed in the MTDSC curves for the formulations containing the highest proportion of ITZ (~35%; formulations F1, F3, and F4) (Fig. 1). The glass transition at about 49°C was present in the reversing heat flow, as was the cold crystallization exotherm at around 100°C in the non-reversing heat flow. These thermal events were not detected in the formulations containing the smallest proportion of ITZ (~10%, formulations F2 and F5), most likely due to the lack of sensitivity of the thermal detection method. The spray-dried mannitol and ITZ melted (total heat flow) at around the same temperature (i.e., 164°C). One supplementary endothermic peak followed by an exothermic peak around 150°C was observed for

Table II Physicochemical Characterization of the Dry Powders for Inhalation: ITZ Content (mean ± S.D., *n*=5), Weight Loss Measured by TGA (mean ± S.D., *n*=3), Amorphous Content, and α-, β- and δ- Mannitol, as Measured by PXRD, Are Shown

Formulation	Drug content				TGA	PXRD			
	Measured ITZ content (wt%)	Coefficient variation (%)	Expected ITZ content (wt%)	Relative error (%)	Weight loss (%)	Amorphous content (%)	α-mannitol (%)	β-mannitol (%)	δ-mannitol (%)
F1	34.5 ± 0.6	1.64	35.9	−3.9	0.35 ± 0.05	55	42	2.5	55.1
F2	10 ± 0.3	3.25	10	−0.1	0.35 ± 0.03	34.5	38.3	1.3	60.3
F3	35.6 ± 0.7	1.82	35.8	−0.6	0.30 ± 0.04	53	31.4	2.9	65.7
F4	33.6 ± 0.7	2.01	34.65	−3.1	0.19 ± 0.2	57	1.1	0.4	98.5
F5	10.2 ± 0.2	1.98	9.9	3.0	0.17 ± 0.04	37	20.5	0.9	78.8
Spray-dried ITZ[a]	100.7 ± 1.6	1.61	100	0.7	–	100	–	–	–
Spray-dried Mannitol[a]	–	–	–	–	–	22.9	77.9	4.1	18

[a] spray-dried in the same conditions as formulations F1, F2, F3, F4, and F5

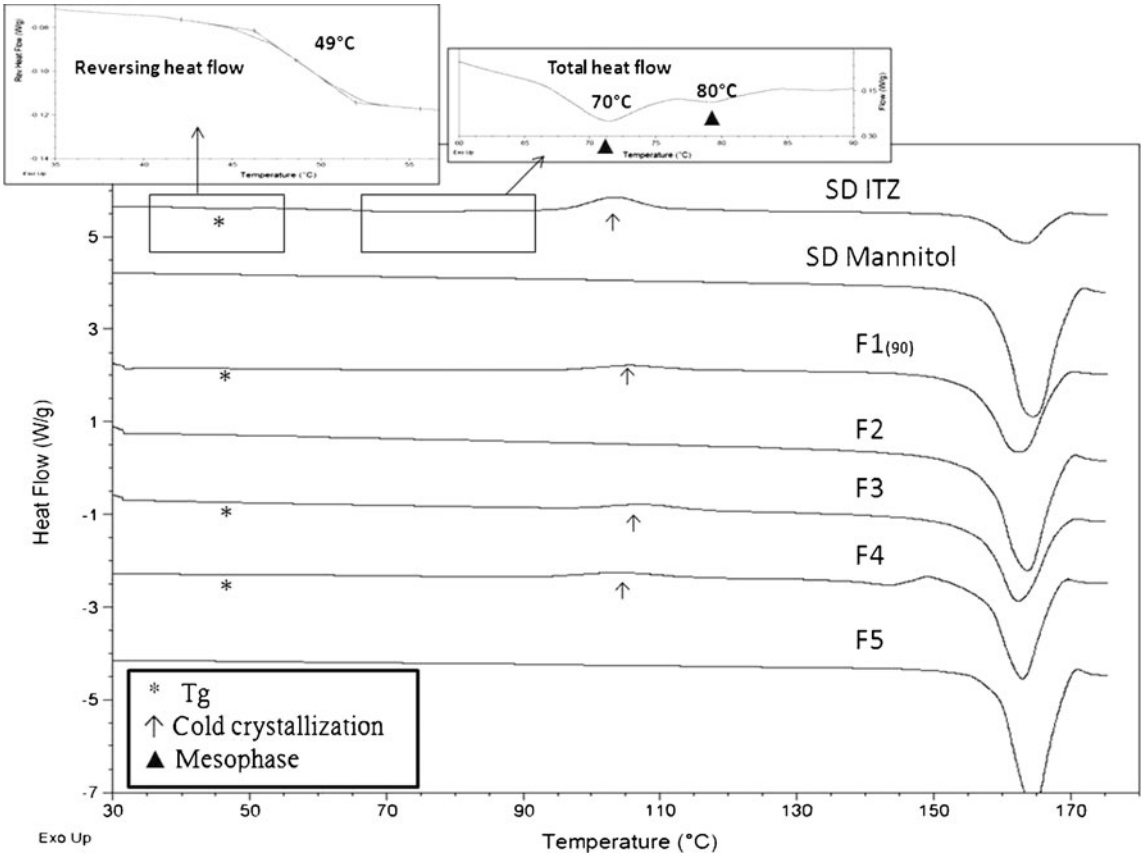

Fig. 1 MTDSC heating curves for spray-dried ITZ, mannitol, and the dry powder formulations (exothermic events are up).

formulation F4. These transitions correspond to the melting of δ-mannitol followed by crystallization into the β-polymorph (25). The other formulations did not exhibit this thermal event, most likely because the mannitol was almost completely in the δ form in formulation F4 (see below).

The PXRD patterns are illustrated in Fig. 2. The characteristic halo spectrum of an amorphous compound was observed for the pure spray-dried ITZ. The amorphous content calculated for this sample was equal to 100% (Table II), which confirmed the lack of any crystalline structure. The pure spray-dried mannitol was mostly in the crystalline form, which is in agreement with other previously published works (25,26). Diffraction peaks corresponding to the crystalline material were present in all of the solid dispersion formulations (Fig. 2). The diffraction peaks for ITZ positioned at 4.62° 2θ, 8.69° 2θ, 14.5° 2θ, which are angular positions where no crystalline mannitol polymorph diffract, were selected as indicators of the ITZ crystalline state. These particular peaks were not present in any of the formulations, which suggested the amorphous nature of ITZ. No diffraction peaks characteristic of PL were visible in the formulations containing the surfactant agent (formulations F3, F4, and F5), most likely due to the very low proportion and likely amorphous nature of PL after spray-drying (27). The amorphous content of the dry powder was determined using the diffractogram surface area ratio method. The results are summarized in Table II. As expected, pure spray-dried mannitol was mostly crystalline, with an estimated amorphous content of 22.9%. The amorphous percentages calculated for all of the formulations were in accordance with their measured ITZ content, theoretical PL content, and the estimated content of amorphous spray-dried pure mannitol. For instance, the ITZ content measured for formulation F1 was equal to 34.5%, while pure mannitol spray-dried at the same concentration showed an amorphous content of 22.9%. If ITZ had been entirely amorphous in F1, a total amorphous content of 57.4% would have been calculated, whereas the actual amorphous content was estimated to be 55%. The sum of the ITZ content measured by HPLC (Table II) and the theoretical PL content (Table I) of all of the respective formulations (expressed as % w/w) were strongly correlated with the amorphous content calculated by PXRD (R^2=0.99, Fig. 3). This finding indicated that an increase in the content of ITZ and PL was accompanied by a proportional increase in the amorphous content of the dry powders. Coupled with the MTDSC results, this finding suggested that ITZ and PL were entirely amorphous in those formulations and that the diffraction peaks only came from crystalline mannitol. No evidence of either amorphous ITZ or PL recrystallization was observed in any of the formulations after 1 year of storage, and the percentage of amorphous content remained unchanged (data not shown).

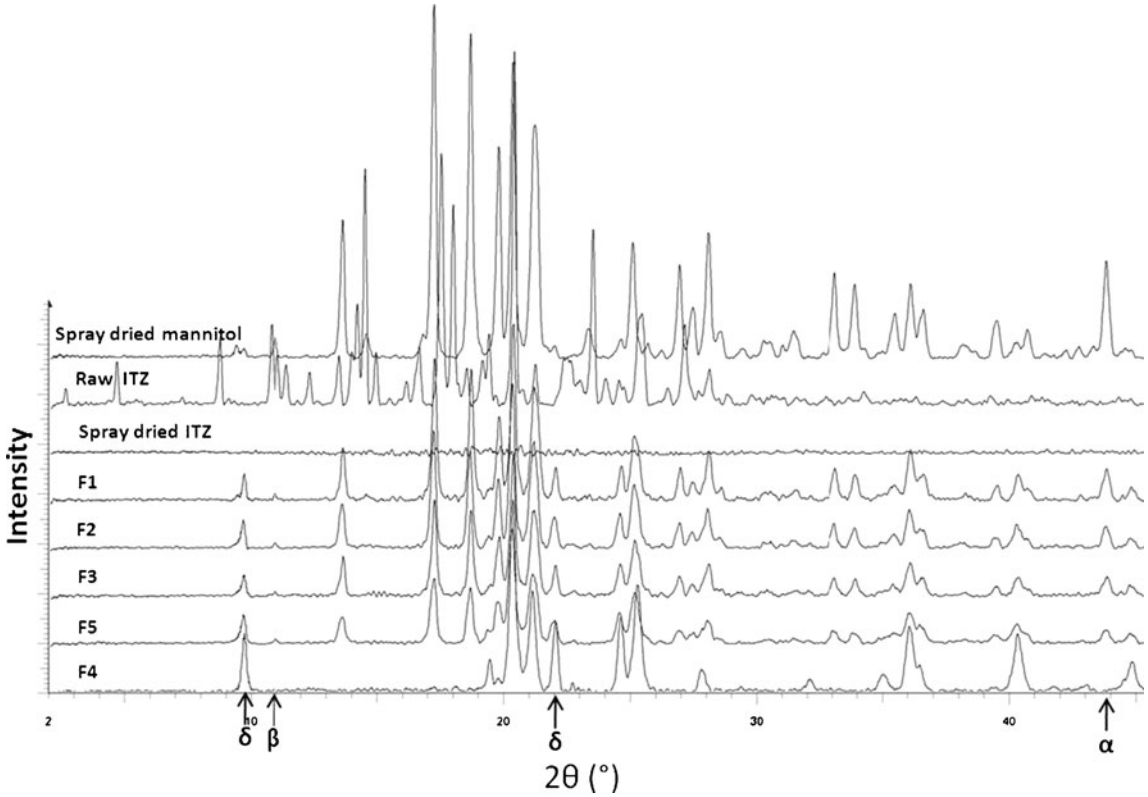

Fig. 2 PXRD diffractograms for raw ITZ, spray-dried ITZ, and the dry powder formulations.α, β, and δ-mannitol specific diffractions rays are shown by an arrow.

Mannitol is known to show polymorphisms. The polymorphic form that can be obtained after a formulation process is influenced by the processing conditions and the addition of other components, such as proteins (25,28). Three particular crystalline polymorphs have been widely described in the literature (29) and are classified as the α-, β-, and δ-polymorphs. These polymorphs are reported to present different PXRD patterns, with specific diffraction peaks identified for each specimen. The proportion of each polymorph in the total mannitol crystalline network of each formulation was estimated using RIR methodology and used as an inter-formulation comparator. The three mannitol polymorphs were present in all of the spray-dried powders, as judged by comparison to the ICDD reference diffractograms. β-mannitol, which is thermodynamically the most stable polymorph, is recovered in the majority of powders spray-dried from an aqueous solution (30). However, for these particular solid dispersion preparations and even the mannitol that was spray-dried alone, the β-polymorph was in the minority, with relative percentage values ranging from 0.4% to 4.1% (Table II) and the α and δ meta-stable forms becoming the most prevalent polymorphs. The isopropanol seemed to play a role in the formation of the mannitol crystal structure, promoting the nucleation of the mannitol in the form of its α- and δ-polymorphs. On one hand, the more rapid evaporation time from hydro-alcoholic solutions compared to pure water solutions led to the formation of a less stable form because less time was available for the molecules to arrange in the more stable configuration. Indeed, as described by Ostwald (31) the phenomenon of crystallization from a solution starts with a thermodynamically unstable phase that is followed by recrystallization to a thermodynamically more stable phase. Thus, the increase in the drying rate for the isopropanol-water system prevented the reconversion of mannitol to its thermodynamically more stable phase, a process that had enough time to occur in the spray-dried aqueous

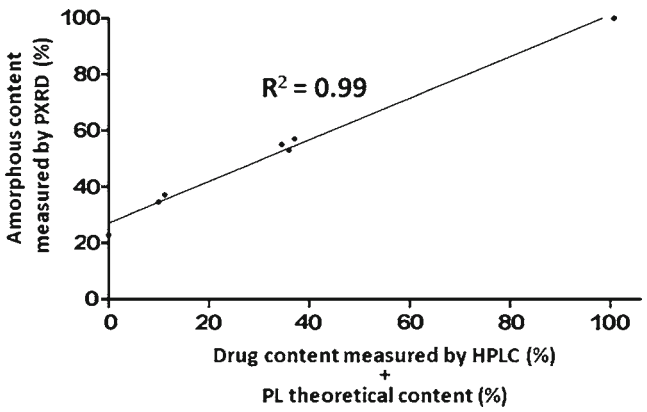

Fig. 3 The correlation between the ITZ content (measured by HPLC) and theoretical PL content (%) and amorphous content, as calculated using PXRD.

systems. On the other hand, solvent molecules can be selectively adsorbed onto the surface of certain polymorphs, thereby either inhibiting their nucleation or retarding their growth to the advantage of others, as demonstrated by Khoshkhoo and Anwar (32). Because mannitol and isopropanol possess many hydrogen acceptor and donor sites (33), hydrogen orientation due to hydrogen bonds is likely to occur between them while isopropanol is adsorbed on mannitol particle surfaces, which influences the crystal orientation during crystal formation. The proportion of α- and δ-polymorphs in the different formulations varied depending on the PL/ITZ/mannitol ratio. Indeed, when comparing pure spray-dried mannitol and formulation F1, the addition of ITZ increased the percentage of the δ-polymorph from 18% to 55.1%. The addition of PL also induced the preferential formation of the δ-mannitol polymorph. During the concomitant spray-drying of mannitol, PL, and ITZ, the latter two most likely promoted the formation of δ- and α-mannitol polymorphs at a molecular level by interacting with their chemical groups (e.g., the highly nucleophilic tertiary amine from the azole group of ITZ), which are also rich in hydrogen bonding sites from the crystallization step. These interactions seemed to favor the preferential orientation of the crystal lattice in the δ-mannitol configuration. The rate of δ-mannitol formation seemed to be correlated with the total amount of PL (Table II). The higher the total amount of PL, the higher the proportion of the δ-polymorph observed (e.g., formulations F1 (0% PL), F3 (0.36% PL), and F4 (3.47% PL) showed δ-mannitol proportions of 55.1%, 65.7%, and 98.5%, respectively). Despite their theoretically lower thermodynamic stability, the δ- and α-mannitol polymorphs did not spontaneously re-crystallize to the β configuration during storage at ambient temperature and humidity conditions (data not shown). This transition is known to occur when the residual moisture in the crystal lattice is elevated (33). Therefore, the lower water content of the sample (<0.5%, Table II) may inhibit polymorphic δ– β conversion.

SEM was used to conduct a qualitative morphological evaluation of the dry powders. Mannitol was the major component of the spray-dried formulations and was therefore subject to forming matricial particles, within which the ITZ and PL (when applicable) were dispersed. Representative SEM micrographs are illustrated in Fig. 4. As shown in Fig. 4, spherical structures (approximately 0.25–2 μm in diameter) were obtained from the spray-dried solutions containing mannitol and ITZ (formulations F1 and F2). Formulation F2 seemed to be composed of slightly larger spherical particles, but no other morphological differences were observed between these formulations, despite the different proportions of amorphous content and mannitol polymorphs. The presence of PL induced the formation of larger particles with rough surfaces. This rough appearance was the most pronounced in the formulation with the highest PL content (formulation F4), and interparticular links were observed. Those links were most likely formed during the spray-drying process due to the softening or melting of PL, which has a transition temperature around 54°C (27). Reducing the PL content (formulations F3 and F5) considerably reduced the interparticular links as well as the surface irregularities. Nevertheless, the core structure of these particles was homogeneous. In contrast with the polymeric surfactant used previously (15), PL seemed to be well distributed within the mannitol particles. This type of homogeneity between mannitol and phospholipids after spray-drying has already been demonstrated (34).

The flow properties of the dry powder formulations were evaluated by determining the Carr's compressibility index (CI), which is frequently used to measure powder flowability (27,35). Good powder flowability is a necessary characteristic for easy processing at an industrial scale. More specifically for DPI, good flowability has already been related to generating adequate metering, dispersion, and fluidization of a dry powder from an inhaler device. All of the formulations exhibited CI values between 15.6% and 26.4% (Table III), which indicated good potential flow properties for this type of formulation. On one hand, a reduction in ITZ content improved the flow properties. Indeed, reducing the ITZ content from 34.5% (formulation F1) to 10.0% (formulation F2) decreased the CI value from 26.4% to 20.6%. A higher ITZ content induced a higher degree of amorphous content and reduced powder flowability, most likely by enhancing interparticular adhesion. Powders with high amorphous content exhibit high surface energy, which leads to a rise in interparticular forces and the adsorption of water and creates supplementary capillary interparticular forces (36,37). On the other hand, an improvement in flow properties was observed with the introduction of PL (CI of 26.4% and 18.1% for formulations F1 and F3, respectively), which potentially reduces particle surface energy and water sorption and therefore cohesion (38). Additionally, PL induced surface irregularities and particle size growth that could increase the inter-particle distance and decrease the total surface area, thereby reducing the inter-particular interactions. However, the improvement for formulation F4, which contains the highest PL content, was very low. This lack of improvement was most likely due to the tendency for the particles to stick together and/or the greater mechanical interlocking arising from their higher morphological irregularity, which negatively affect flowability.

Particle Size Analysis and Aerodynamic Behavior

The principal advantage of an inhalation-based therapeutic approach for the treatment of pulmonary IA is being able to administer the entire dose of antifungal agent directly to the site of infiltration without systemic exposure. However, the efficacy of antifungal agents depends on their concentration

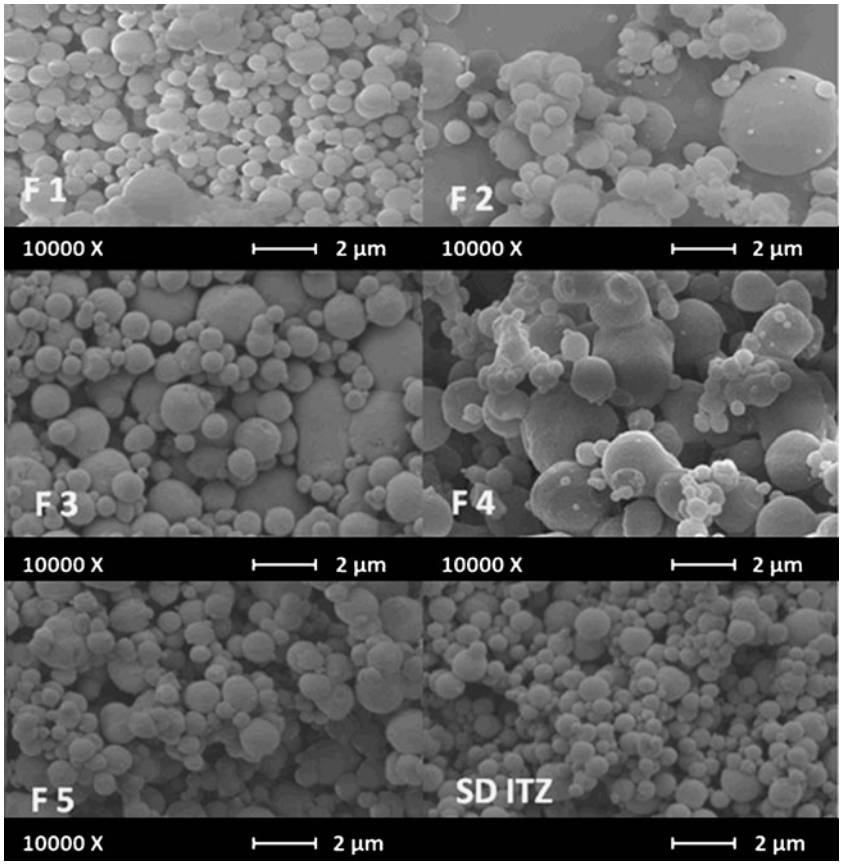

Fig. 4 SEM photographs of the spray-dried ITZ (SD ITZ) and the dry powder formulations (F1, F2, F3, F4, and F5) at magnifications of 10 000X.

at the site of fungal growth. Antifungals have a minimal concentration at which *in vitro* activity is optimal for inhibiting fungal growth. Therefore, theoretically, the post-inhalation concentration of ITZ inside a fungal lesion should not be below a determined concentration if one wishes to attain a positive outcome from the treatment (fungal hyphae eradication). A plasmatic concentration of less than 500 ng ITZ/ml after oral or intravenous administration to immunocompromised patients carried a significantly increased risk of invasive yeast (mainly pulmonary aspergillosis) (39), which confirmed a strong inverse relationship between the plasma concentration of ITZ and the pulmonary burden of IA in a preclinical study (40). Those plasma concentration/activity relationships were most likely secondary to the ITZ concentration present in lung fungal lesions when increasing the plasma concentration, which is known to induce pronounced adverse reactions and systemic interactions. Several of the studies that used murine models of pulmonary IA that delivered antifungals directly into the lungs by nebulization suggested such a relationship. A minimum concentration of 2 µg/g of lung tissue corresponds to the ITZ

Table III Size, Aerodynamics, and Flow Characteristics of Formulations F1, F2, F3, F4, and F5: Particle Size Characteristics (mean ± SD, $n=3$) Measured by the Mastersizer 2000® and the Spraytec®, the Emitted Dose (ED, Expressed in % of nominal dose), Dose Recovery (% of nominal dose, $n=3$), Fine Particle Fractions (FPF, % of particle with $d_{ae} < 5$ µm expressed in function of nominal dose) Measured by an Impaction Test (mean ± SD, $n=3$), and Carr's Index Value (CI, mean ± SD, $n=3$) Are Shown

Formulation	Laser light scattering				Aerodynamic evaluation				Flow properties
	Mastersizer 2000®		Spraytec®		MsLI				
	d(0.5) (µm)	D[4,3] (µm)	d(0.5) (µm)	D[4,3] (µm)	ED ($\%_{nom}$)	FPF_{nom} ($\%_{nom}$)	FPD (mg)	Dose recovery (%)	CI (%)
F1	0.74 ± 0.01	1.00 ± 0.04	2.2 ± 0.1	2.8 ± 0.4	53.3 ± 1.9	46.9 ± 1.9	1.17 ± 0.05	87 ± 1	26. ± 0.1
F2	0.88 ± 0.07	1.15 ± 0.05	2.71 ± 0.08	3.66 ± 0.07	81.9 ± 0.6	67.0 ± 1.0	1.68 ± 0.03	92 ± 2	20.6 ± 0.8
F3	1.35 ± 0.01	1.59 ± 0.01	2.97 ± 0.04	3.14 ± 0.08	68.3 ± 7.8	52.5 ± 4.9	1.31 ± 0.2	87 ± 1	18.1 ± 2.1
F4	1.81 ± 0.05	2.04 ± 0.05	4.63 ± 0.01	5.27 ± 0.07	75.2 ± 4.6	43.0 ± 5.2	1.08 ± 0.13	90 ± 4	24.9 ± 0.9
F5	0.93 ± 0.01	1.23 ± 0.04	3.14 ± 0.09	3.93 ± 0.40	84.9 ± 5.3	66.4 ± 3.6	1.66 ± 0.09	95 ± 4	15.6 ± 1.9

MIC for the strain in question (2 μg/ml is the MIC 90% for ITZ against *Aspergillus fumigatus*, (41)) and was proven effective in survival studies (6,7). Therefore, an "efficient" human lung dose could be extrapolated from those encouraging data. A human lung weighs approximately 200–300 g, which is approximately 0.35% of the total body weight (42). The initial lung dose administered should therefore be higher than 300 g×2 μg (600 μg) to achieve a pulmonary ITZ concentration higher that 2 μg/g of lung. But, one remaining issue is where to deposit the powder dose. Due to their small d_{ae} (e.g., d_{ae} ~3 μm for *A. fumigatus*, (21)), *Aspergillus* conidia are able to penetrate deep into the lung. The ITZ particles generated from an inhaler device must penetrate as deeply as the inhaled conidia (to where hyphal proliferation could take place), and the d_{ae} ~3 μm fraction must be maximized. Therefore, the FPD could be taken as an indicator of the probable dose that will reach the fungal lesions after inhalation. PSD analyses and MsLI tests were conducted on all of the formulations to determine the formulations' particle sizes and the ITZ FPD after emission from an inhaler device. The results are summarized in Table III. The deposition patterns are expressed as a percentage of the nominal dose in Fig. 5.

The Malvern Mastersizer 2000® results showed that all of the formulations presented a very fine PSD, with a mean volume diameter D[4,3] ranging from 1.00 μm to 2.04 μm and a median volume diameter d(0.5) ranging between 0.74 μm and 1.81 μm (Table III). The PSDs of the formulations without PL (formulations F1 and F2) were very close, with d(0.5) values of 0.74 μm and 0.88 μm, respectively. However, as observed by SEM, a small proportion of the particles formed in formulation F2 were larger, which corresponded to slightly higher D[4,3] and d(0,5) values. Interestingly, this formulation possessed a higher δ-mannitol proportion than formulation F1, as previously described. A different nucleation process resulting from a different crystalline structure could explain this appearance of larger particles during the crystallization that followed the evaporation of solution droplets (33). This observation is supported by the fact that the addition of 1% (formulation F3) and 10% (formulation F4) PL, expressed by weight of ITZ, raised the δ proportion from 55.1% (0%, formulation F1) to 65.7% and 98.5%, respectively. This increase in the δ proportion was also followed by an increase in particle size (formulations F1, F3, and F4 presented D[4,3] values of 1.00, 1.59, and 2.04 μm, respectively). Similar observations were made when comparing formulation F2 (0% PL) and formulation F5 (10% PL w/w_{ITZ}). The particle sizes seemed to be directly influenced by the proportion of mannitol in the δ crystalline form, which is itself influenced by the PL content in the formulation. This result is in complete agreement with Lee *et al.* (43), who have recently demonstrated a relationship between the amounts of α- and β-mannitol and particle size. This relationship between mannitol polymorphism and PSD was also observed when measuring the particle size of the formulation's dry powder aerosol after emission from a dry powder inhaler. Figure 6 clearly shows that the percentage of δ-mannitol present correlated very well with the particle size measured with the Spraytec®. This was equally true for the α- and β-mannitol polymorph percentages. We can therefore assume that the variations in mannitol polymorph modified the formulations' aerodynamic behavior by forming particles with different sizes that depended on the proportions of the α-, β-, and δ-polymorphs.

The targeted FPD of 600 μg was reached in each formulation with a nominal ITZ dose of 2.5 mg. Thus, the correct dose of ITZ should theoretically be administered after inhalation by a patient. However, since the nineties, multi azole resistant *Aspergillus* species have progressively emerged (44). This resistance is associated with a higher MIC. Therefore, the administration of higher ITZ doses should be considered to minimize the resistance phenomenon. A recent prospective study in Denmark outlined this problem while evaluating the susceptibility pattern of aspergilli in human airway samples (45). Considering (i) that ITZ resistant strains present an MIC > 2 μg/ml (46) and (ii) the recently defined itraconazole MIC of 4 μg/ml for clinical and environmental isolates of *Aspergillus* species (47)

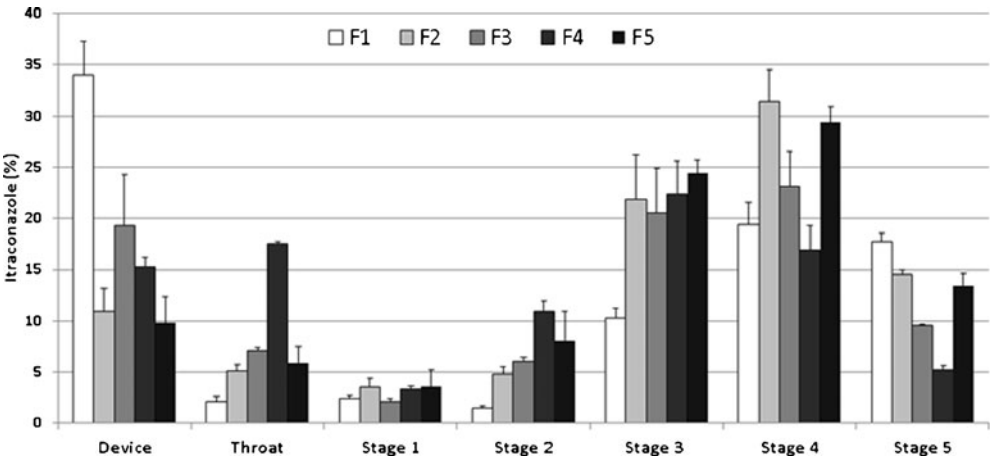

Fig. 5 The *in vitro* deposition patterns (mean ± S.D, *n*=3) of the dry powder formulations were determined with an MsLI from the Axahaler® device. The following conditions were used: 100 L/min, 2.4 s. Three n° 3 HPMC capsules were filled with a quantity of formulation corresponding to 2.5 mg of itraconazole and used in each test. The percentages of itraconazole are expressed as a function of the nominal dose.

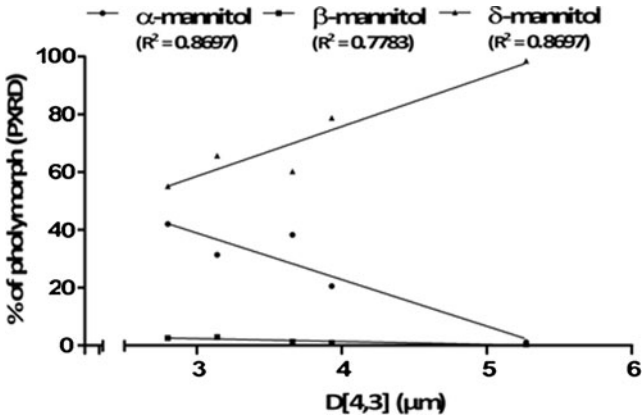

Fig. 6 The correlation between the % of each mannitol polymorph measured by PXRD and the respective D[4,3] (in μm) of each formulation, as measured by Spraytec®.

the targeted lung dose should therefore be higher than 300 g × 4 µg (1.2 mg) to achieve effective pulmonary ITZ concentrations high enough to allow *Aspergillus* resistance to be overcome.

The FPDs of the formulations ranged from 1.08 ± 0.13 mg to 1.68 ± 0.03 mg, which correspond to 1–1.4 times the targeted FPD. These values corresponded to FPFs (expressed as a function of the nominal dose) ranging from 43% to 67%, which is relatively high compared to the low FPF values of marketed DPI (i.e., 30–40%). The ED of the formulations varied from 53.3% to 84.9% (Table III), and two major trends were clearly observed. There were considerable improvements in device and capsule emptying when the ITZ content decreased and when PL was introduced into the formulation. The reduction in drug content from 34.5% (formulation F1) to 10% (formulation F2) increased the ED from 53.3% to 81.9%, which considerably increased the FPD from 1.17 mg to 1.68 mg. When comparing formulations with equivalent drug content, the increase in PL content (w/w) from 0% (formulation F1) to 0.36% (formulation F3) and 3.47% (formulation F4) improved the ED to 15% and 21.9%, respectively. However, formulation F4, which showed a superior ED in comparison with formulations F1 and F3 (due to a PL content of 3.47% w/w), exhibited the lower FPD. This trend was likely to have been observed, as judged by the increase in particle size that was induced by the increased PL content associated with polymorphic variation. Indeed, as previously described, formulation F4 exhibited the largest particle size. As depicted in Fig. 5 (and despite the higher ED of formulation F4 compared to formulations F1 and F3), a lower fraction of the ITZ in formulation F4 reached stages 3 and 4 and the filter of the impactor because of massive particle impaction on the throat and a higher impaction rate on stage 2 of the MsLI. Thus, the introduction of PL improved device emptying for formulation F4. However, the increase in particle size caused a high proportion of the emitted dose to be stopped in the upper parts of the impactor, which reduced the FPD in comparison with the formulations containing less or no PL (F1 and F3). This effect was also observed for formulation F3 (*vs.* formulation F1) and formulation F5 (*vs.* formulation F2), but to a lower extent. However, their FPDs were not extensively modified. Despite the higher impaction rates for formulations F3 and F5 in the upper stages of the impactor (*vs.* their respective comparators), a moderate increase in particle size caused the higher emitted fractions to overcome this

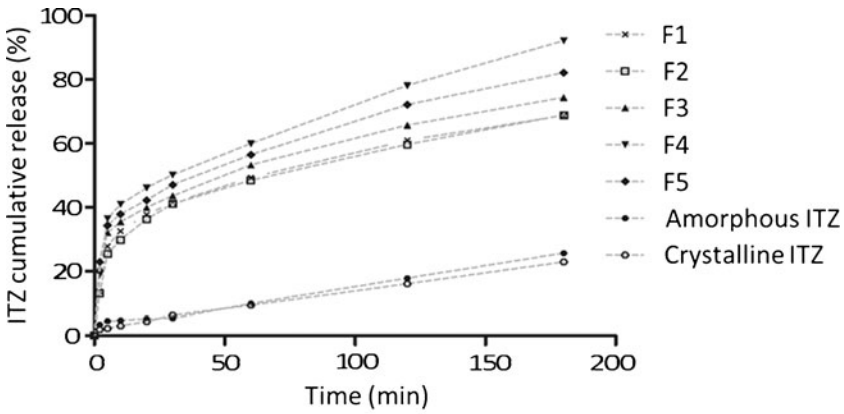

	2	5	10	20	30	60	120	180
F1	13.7±3.4	27.8±4.3	32.5±3.7	37.7±2.6	41.3±1.6	49.2±0.5	60.9±1.9	68.6±4.7
F2	13.1±1.4	25.4±3.5	29.8±2.9	36.2±3.5	41.0±4.6	48.4±1.1	59.6±4.8	68.8±4.5
F3	21.1±2.1	32.0±3.4	35.4±3.5	39.9±3.7	43.5±4.0	53.2±3.6	65.6±4.1	74.3±4.9
F4	18.9±0.5	36.4±0.8	40.9±0.6	46.0±0.39	50.1±0.6	59.9±1.1	78.0±1.3	92.0±1.8
F5	22.9±0.1	34.3±0.6	37.9±0.6	42.1±1	47±0.1	56.4±0.4	72.0±0.2	82±0.4
Crystalline ITZ	1.9±0.6	2.3±0.5	3.0±0.8	4.4±0.9	6.3±2	9.4±0.9	16.0±1.6	22.9±1.4
Amorphous ITZ	3.4±0.3	4.5±0.3	4.7±0.1	5.2±0.2	5.4±0.7	9.9±0.3	17.8±0.9	25.6±1.2

Fig. 7 *In vitro* dissolution profiles of crystalline (raw) and amorphous (spray-dried) itraconazole and the five dry powder formulations. These profiles were determined after impaction (NGI with an Axahaler® device at 60 L/min, 4 s, n°3 HPMC capsule) of the quantity of dry powder corresponding to 400 μg of itraconazole (d_{ae}: 2.82–4.46 μm) on a membrane cassette that was then placed into the vessel of a USP 33 type II apparatus (300 ml of dissolution media, pH 7.2 + 0.3% sodium lauryl sulfate, 37°C, paddle speed rotation, 75 rpm).

Table IV Statistical Analysis of the Itraconazole Release Profiles Obtained During the Dissolution Tests: Difference (f_1) and Similarity (f_2) Fit Factors were Calculated for Each Pair of Curves. f_1 <15 and f_2 >50 Suggested Statistical Equivalence Between Two Curves

Investigated characteristic	Reference	Test	Similarity (f_2) (similar : $f_2 > 50$)	Difference (f_1) (different: f_1 >15)	Conclusion
ITZ amorphization	Crystalline (ITZc)	Amorphous (ITZa)	85.64	5.62	Equivalent
Dissolution improvement	ITZc	F1	22.91*	80.07*	Not equivalent
	ITZc	F2	23.55*	79.49*	Not equivalent
	ITZc	F3	20.62*	81.88*	Not equivalent
	ITZc	F4	16.37*	84.34*	Not equivalent
	ITZc	F5	18.46*	83.24*	Not equivalent
Formation of matricial particles	ITZa	F1	23.68*	76.97*	Not equivalent
	ITZa	F2	24.34*	76.29*	Not equivalent
ITZ content (% w/w)	10 (F2)	35.9 (F1)	86.89	2.94	Equivalent
% phospholipids (% w/w)	0 (F1)	0.36 (F3)	66.98	9.70	Equivalent
	0 (F1)	0.99 (F5)	53.7	15.91*	Not equivalent
	0 (F2)	0.99 (F5)	51.29	18.31*	Not equivalent
	0 (F1)	3.47 (F4)	44.91*	21.40*	Not equivalent
	0.36 (F3)	0.99 (F5)	68.10	8.13	Equivalent
	0.36 (F3)	3.47 (F4)	52.15	15.69*	Not equivalent
	3.47 (F4)	0.99 (F5)	64.53	6.99	Equivalent

impacted fraction and allowed supplementary particle penetration into the lower stages of the impactor, thus balancing the loss in the upper parts. Formulations F2 and F5 showed the best aerodynamic properties, with very high FPDs of 1.68 mg and 1.66 mg, respectively.

Dissolution Test

Dissolution tests were conducted to compare the API dissolution release from the different formulations. It is important to note that there is currently no standardized pharmacopoeia *in vitro* dissolution method specifically designed for measuring the dissolution of a dry powder for inhalation. In this study, we used a recently developed dissolution test that is based on the collection of a determined aerodynamic particle range on an impactor plate. This method has already been successfully used to evaluate the release profile of a dry powder for inhalation (48). In our specific context, this technique presents several advantages. Indeed, only the fraction of the dry powder that presents the same d_{ae} as inhaled conidia would be evaluated in terms of dissolution rate. This aerodynamic selection also limits the variation that the PSD imparts on the dissolution kinetic of the active ingredient. Moreover, once inhaled, particle dissolution would occur in a system that is stagnant rather than well-stirred, and this technique is based on a dissolution diffusion system, allowing drug dissolution in a passive system that could mechanically mimic dry powder dissolution after lung deposition.

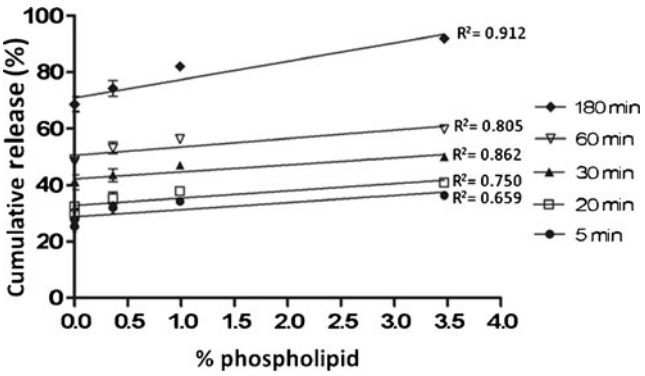

Fig. 8 Percentage of the cumulative release as a function of the quantity of PL in the formulations at 5, 30, and 60 min (F1 (0% PL), F2 (0% PL), F3 (0.36% PL), F4 (3.47% PL), F5 (0.99% PL)).

The *in vitro* release profiles obtained are shown in Fig. 7. Pairs of curves were chosen to investigate the influence of particular formulation characteristics on the dissolution behavior of ITZ. The influence of the amorphization of the API, the formation of matricial particles, the active drug payload, and the addition of surfactant in the formulation were investigated. The corresponding calculated fit factors that are statistically indicated for pairs of curves are summarized in Table IV.

All of the formulations showed a faster dissolution rate than raw crystalline ITZ (Fig. 7), a finding that was confirmed by statistical analysis using fit factors (Table IV). A comparison of the dissolution curves of crystalline and amorphous ITZ suggested no difference in the drug release curves. This observation was interesting because amorphous ITZ would be expected to have a faster dissolution profile than crystalline ITZ (49). This effect may be because the highly hydrophobic

nature of the drug substance could lead to poor wettability by the aqueous dissolution media, impeding any improvement in drug dissolution. The progressive re-crystallization of amorphous ITZ could also have occurred during dissolution, delaying the dissolution of the amorphous form. However, when dispersed in mannitol microparticles (formulations F1 and F2), a significant improvement in the dissolution rate of ITZ was observed ($f1 > 15$ and $f2 < 50$, Table IV). Mannitol formed a spherical matrix in which the amorphous ITZ particles were dispersed. Because mannitol dissolves almost instantly, it was assumed that the amorphous ITZ particles exposed a higher surface area to the dissolution media than the pure spray-dried ITZ, leading to a faster dissolution rate. No difference in dissolution performance was observed when the ITZ content decreased from 35.4% (formulation F1) to 10.0% (formulation F2) (Table IV, Fig. 7). This result emphasizes the flexibility that this formulation strategy offers as the aerodynamic performance of F2 was considerably improved compared to F1. For an ITZ content of up to 35%, the wettability is enhanced by the formation of a solid dispersion (Table IV, Fig. 7).

The addition of PL to the formulation (formulations F3, F4, and F5) accelerated the ITZ dissolution rate (Fig. 8). Due to its amphiphilic structure, PL most likely helped to improve the wettability of the hydrophobic ITZ in the aqueous media. This better wettability most likely created a microenvironment in which the ITZ saturation concentration was enhanced around the dissolving particles, accelerating its dissolution rate. The accelerating effect of PL on ITZ dissolution rate was strikingly clear from the graph (Fig. 7). Increasing the PL content gradually accelerated ITZ dissolution, with a faster release rate for formulation F4, which contained the highest PL content. The linear regression of the percentage of PL in the dry form *versus* the percentage of release at different time points exhibited good correlations (Fig. 8). This finding indicates that increasing the PL content proportionally accelerates the ITZ dissolution rate and suggests a good distribution of PL into the solid dispersion, which gives wetting enhancement activity that is accentuated when the PL content is increased. Because the ITZ dissolution rate was accelerated by particle PL content and PLs are known to improve drug permeation, the different formulations are therefore likely to provide different *in situ* pharmacokinetic profiles.

CONCLUSION

In this study, we showed that ITZ-based dry powders for inhalation can be developed to have acceptable inhalation excipients, optimized aerodynamic performance, and modulated release properties. Indeed, ITZ-based solid mannitol dispersions with or without phospholipids were found to be suitable for delivering ITZ to the lung while enhancing its dissolution properties. The best formulation for the inhaled treatment of invasive pulmonary aspergillosis is F5, which contained 10% PL (by weight of ITZ) and exhibited the fastest dissolution profile and aerosol performances with a high ED (81.9%). These good dispersion and high FPD (1.68 mg) characteristics suggest a formulation that can achieve the theoretical targeted pulmonary ITZ dose of 1.2 mg and overcome a potentially resistant *Aspergillus* strain. In the future, a pharmacokinetic assessment of the dry powders for inhalation will be performed by intratracheal insufflation to determine the optimal formulation for maintaining an ITZ MIC 90% in the lungs. Based on these results, an *in vivo* efficacy study will be conducted.

REFERENCES

1. Mcneil MM, Nash SL, Hajjeh RA, Phelan MA, Conn LA, Plikaytis BD, Warnock DW. Trends in mortality due to invasive mycotic diseases in the United States, 1980–1997. Clin Infect Dis. 2001;33:641–7.
2. Denning DW. Invasive aspergillosis. Clin Infect Dis. 1998;26:781–803.
3. Hope WW. Invasion of the alveolar-capillary barrier by Aspergillus spp.: therapeutic and diagnostic implications for immunocompromised patients with invasive pulmonary aspergillosis. Med Mycol. 2009;47 Suppl 1:S291–8.
4. Hope WW, Billaud EM, Lestner J, Denning DW. Therapeutic drug monitoring for triazoles. Curr Opin Infect Dis. 2008;21:580–6.
5. Coronel B, Levron JC, Dorez D, Van Devenne A, Archimbaud E, Mercatello A. Itraconazole lung concentrations in haematological patients. Mycoses. 2000;43:125–7.
6. Hoeben BJ, Burgess DS, McConville JT, Najvar LK, Talbert RL, Peters JI, Wiederhold NP, Frei BL, Graybill JR, Bocanegra R, Overhoff KA, Sinswat P, Johnston KP, Williams RO. *In vivo* efficacy of aerosolized nanostructured itraconazole formulations for prevention of invasive pulmonary aspergillosis. Antimicrob Agents Chemother. 2006;50:1552–4.
7. Alvarez CA, Wiederhold NP, McConville JT, Peters JI, Najvar LK, Graybill JR, Coalson JJ, Talbert RL, Burgess DS, Bocanegra R, Johnston KP, Williams RO. Aerosolized nanostructured itraconazole as prophylaxis against invasive pulmonary aspergillosis. J Infect. 2007;55:68–74.
8. Chan HK. Dry powder aerosol delivery systems: current and future research directions. J Aerosol Med. 2006;19:21–7.
9. Amidon GL, Lennernas H, Shah VP, Crison JR. A theoretical basis for A biopharmaceutic drug classification—the correlation of *in-vitro* drug product dissolution and *in-vivo* bioavailability. Pharm Res. 1995;12:413–20.
10. Yang W, Tam J, Miller DA, Zhou J, McConville JT, Johnston KP, Williams RO. High bioavailability from nebulized itraconazole nanoparticle dispersions with biocompatible stabilizers. Int J Pharm. 2008;361:177–88.
11. Tran CL, Buchanan D, Cullen RT, Searl A, Jones AD, Donaldson K. Inhalation of poorly soluble particles. II. Influence of particle surface area on inflammation and clearance. Inhal Toxicol. 2000;12:1113–26.
12. Jones RM, Neef N. Interpretation and prediction of inhaled drug particle accumulation in the lung and its associated toxicity. Xenobiotica. 2012;42:86–93.

13. Bindu MB, Kusum B, Banji D. Novel strategies for poorly water soluble drugs. Int J Pharm Sci Rev Res. 2010;4:76–84.
14. Pilcer G, Amighi K. Formulation strategy and use of excipients in pulmonary drug delivery. Int J Pharm. 2010;392:1–19.
15. Duret C, Wauthoz N, Sebti T, Vanderbist F, Amighi K. Solid dispersions of itraconazole for inhalation with enhanced dissolution, solubility and dispersion properties. Int J Pharm. 2012;428(1–2):103–13.
16. Weers JG, Tarara TE, Clark AR. Design of fine particles for pulmonary drug delivery. Expert Opin Drug Deliv. 2007;4 (3):297–313.
17. Shah B, Kakumanu VK, Bansal AK. Analytical techniques for quantification of amorphous/crystalline phases in pharmaceutical solids. J Pharm Sci. 2006;95:1641–65.
18. Chung FH. Quantitative interpretation of X-ray diffraction patterns of mixtures. II. Adiabatic principle of X-ray diffraction analysis of mixtures. J App Cryst. 1974;7:526–31.
19. Wandt MA, Rodgers AL. Quantitative X-ray diffraction analysis of urinary calculi by use of the internal-standard method and reference intensity ratios. Clin Chem. 1988;34:289–93.
20. Galunin E, Vidal M, Alba MD. The effect of polymorphic structure on the structural and chemical stability of yttrium disilicates. Am Mineral. 2011;96:1512–20.
21. Morris G, Kokki MH, Anderson K, Richardson MD. Sampling of Aspergillus spores in air. J Hosp Infect. 2000;44:81–92.
22. Shah VP, Tsong Y, Sathe P, Liu JP. *In vitro* dissolution profile comparison–statistics and analysis of the similarity factor, f2. Pharm Res. 1998;15:889–96.
23. Weiler C, Egen M, Trunk M, Langguth P. Force control and powder dispersibility of spray dried particles for inhalation. J Pharm Sci. 2010;99:303–16.
24. Miao S, Roos YH. Crystallization kinetics and x-ray diffraction of crystals formed in amorphous lactose, trehalose, and lactose/trehalose mixtures. J Food Sci. 2005;70:E350–8.
25. Hulse WL, Forbes RT, Bonner MC, Getrost M. The characterization and comparison of spray-dried mannitol samples. Drug Dev Ind Pharm. 2009;35:712–8.
26. Elversson J, Millqvist-Fureby A. Particle size and density in spray drying—effects of carbohydrate properties. J Pharm Sci. 2005; 94:2049–60.
27. Sebti T, Amighi K. Preparation and *in vitro* evaluation of lipidic carriers and fillers for inhalation. Eur J Pharm Biopharm. 2006;63:51–8.
28. Kaialy W, Martin GP, Ticehurst MD, Momin MN, Nokhodchi A. The enhanced aerosol performance of salbutamol from dry powders containing engineered mannitol as excipient. Int J Pharm. 2010;392:178–88.
29. Burger A, Henck JO, Hetz S, Rollinger JM, Weissnicht AA, Stottner H. Energy/temperature diagram and compression behavior of the polymorphs of D-mannitol. J Pharm Sci. 2000;89:457–68.
30. Hulse WL, Forbes RT, Bonner MC, Getrost M. Influence of protein on mannitol polymorphic form produced during co-spray drying. Int J Pharm. 2009;382:67–72.
31. Ostwald W. Studien uber die bildung und Umwandlung fester Korper. Z Phys Chem. 1897;22:289.
32. Khoshkhoo S, Anwart J. Crystallization of polymorphs: the effect of solvent. J Phys D: Appl Phys. 1993;26:890–3.
33. Yoshinari T, Forbes RT, York P, Kawashima Y. Moisture induced polymorphic transition of mannitol and its morphological transformation. Int J Pharm. 2002;247:69–77.
34. Alves GP, Santana MHA. Phospholipid dry powders produced by spray drying processing: structural, thermodynamic and physical properties. Powder Technol. 2004;145:139–48.
35. Iida K, Hayakawa Y, Okamoto H, Danjo K, Leuenberger H. Evaluation of flow properties of dry powder inhalation of salbutamol sulfate with lactose carrier. Chem Pharm Bull. 2001;49:1326–30.
36. Larhrib H, Martin GP, Marriott C, Prime D. The influence of carrier and drug morphology on drug delivery from dry powder formulations. Int J Pharm. 2003;257:283–96.
37. Zhang Y, Wang XL, Lin X, Liu XL, Tian B, Tang X. High azithromycin loading powders for inhalation and their *in vivo* evaluation in rats. Int J Pharm. 2010;395:205–14.
38. Bosquillon C, Rouxhet PG, Ahimou F, Simon D, Culot C, Preat V, Vanbever R. Aerosolization properties, surface composition and physical state of spray-dried protein powders. J Control Release. 2004;99:357–67.
39. Glasmacher A, Hahn C, Leutner C, Molitor E, Wardelmann E, Losem C, Sauerbruch T, Marklein G, Schmidt-Wolf IG. Breakthrough invasive fungal infections in neutropenic patients after prophylaxis with itraconazole. Mycoses. 1999;42: 443–51.
40. Berenguer J, Ali NM, Allende MC, Lee J, Garrett K, Battaglia S, Piscitelli SC, Rinaldi MG, Pizzo PA, Walsh TJ. Itraconazole for experimental pulmonary aspergillosis: comparison with amphotericin B, interaction with cyclosporin A, and correlation between therapeutic response and itraconazole concentrations in plasma. Antimicrob Agents Chemother. 1994;38:1303–8.
41. Pfaller MA, Messer SA, Hollis RJ, Jones RN. Antifungal activities of posaconazole, ravuconazole, and voriconazole compared to those of itraconazole and amphotericin B against 239 clinical isolates of Aspergillus spp. and other filamentous fungi: Report from SENTRY Antimicrobial Surveillance Program, 2000. Antimicrob Agents Chemother. 2002;46:1032–7.
42. Osaki T, Hanagiri T, Nakanishi R, Yoshino I, Taga S, Yasumoto K. Bronchial arterial infusion is an effective therapeutic modality for centrally located early-stage lung cancer: results of a pilot study. Chest. 1999;115:1424–8.
43. Lee YY, Wu JX, Yang M, Young PM, van Den BF, Rantanen J. Particle size dependence of polymorphism in spray-dried mannitol. Eur J Pharm Sci. 2011;44:41–8.
44. Snelders E, van der Lee HA, Kuijpers J, Rijs AJ, Varga J, Samson RA, Mellado E, Donders AR, Melchers WJ, Verweij PE. Emergence of azole resistance in Aspergillus fumigatus and spread of a single resistance mechanism. PLoS Med. 2008;5: e219.
45. Mortensen KL, Johansen HK, Fuursted K, Knudsen JD, Gahrn-Hansen B, Jensen RH, Howard SJ, Arendrup MC. A prospective survey of Aspergillus spp. in respiratory tract samples: prevalence, clinical impact and antifungal susceptibility. Eur J Clin Microbiol Infect Dis. 2011;30:1355–63.
46. Verweij PE, Howard SJ, Melchers WJ, Denning DW. Azole-resistance in Aspergillus: proposed nomenclature and breakpoints. Drug Resist Updat. 2009;12:141–7.
47. Misra R, Malik A, Singhal S. Comparison of the activities of amphotericin B, itraconazole, and voriconazole against clinical and environmental isolates of Aspergillus species. Indian J Pathol Microbiol. 2011;54:112–6.
48. Wauthoz N, Deleuze P, Saumet A, Duret C, Kiss R, Amighi K. Temozolomide-based dry powder formulations for lung tumor-related inhalation treatment. Pharm Res. 2011;28:762–75.
49. Six K, Verreck G, Peeters J, Brewster M, Van den Mooter G. Increased physical stability and improved dissolution properties of itraconazole, a class II drug, by solid dispersions that combine fast- and slow-dissolving polymers. J Pharm Sci. 2004;93:124–31.